Structural fire engineering considerations for cross-laminated timber walls

Citation for published version:
Wiesner, F, Hadden, RM, Deeny, S & Bisby, LA 2022, 'Structural fire engineering considerations for cross-laminated timber walls', *Construction and Building Materials*, vol. 323, 126605.
https://doi.org/10.1016/j.conbuildmat.2022.126605

Digital Object Identifier (DOI):
10.1016/j.conbuildmat.2022.126605

Link:
Link to publication record in Edinburgh Research Explorer

Document Version:
Peer reviewed version

Published In:
Construction and Building Materials

Structural fire engineering considerations for cross-laminated timber walls

Felix Wiesner[a, b, *], Rory Hadden[b], Susan Deeny[c], Luke Bisby[b]

[a] School of Civil Engineering, Bldg. 49, Staff House Road, The University of Queensland, Brisbane, QLD, 4072, Australia, f.wiesner@uq.edu.au

[b] School of Engineering, The University of Edinburgh, The King's Buildings, Mayfield Road, Edinburgh, EH9 3JL, Scotland

[c] Arup, 13 Fitzroy Street, London, W1T 4BQ, UK

*Corresponding author

Keywords: Cross-laminated timber; fire safety; buckling; adhesive; tall timber; cooling phase; burnout; fire resistance

Abstract

The current understanding of the thermo-mechanical response of cross-laminated timber (CLT) walls to fire is insufficiently developed. This paper presents results obtained using a novel experimental methodology on fire-exposed CLT walls under sustained loads. The findings demonstrate that global instability is likely to be the dominant failure mode for CLT walls in fire. Use of a polyurethane adhesive resulted in earlier structural failure than use of a melamine urea formaldehyde adhesive. Three-ply walls failed significantly earlier than those with five plies. The combination of these two factors caused a halving of failure time between different walls under identical heating conditions. In addition, CLT walls were found to collapse during artificially induced cooling phases. It is concluded that these findings are centrally relevant considerations for fire design of CLT.

1 Introduction

Cross-laminated timber (CLT) is an engineered wood (mass timber) product consisting of timber boards stacked in alternating grain orientations and held together by polymer adhesives [1, 2]. It is manufactured off-site, which facilitates ease of construction and shorter construction time frames [3, 4]. All CLT mentioned or referred to in this work and in cited literature is arranged so that the wood fibres of the outer boards are aligned in parallel to the main loading direction. The reduced embodied energy in mass timber buildings is considered the key driver for the more widespread adoption of mass timber as the primary structural material in residential and commercial construction [5]. However, since timber is a combustible material, application of mass timber in midrise and high-rise buildings raises concerns regarding its design to ensure adequate fire safety within existing safety frameworks, which originate from assumptions of limited areas of combustible materials as part of the structure [6].

The structural fire safety of buildings has historically been assessed using the widely adopted 'fire resistance' framework, which – regardless of the structural material being used – requires that building elements are able to carry their in-service (i.e. accidental loading case) load whilst being exposed to a standardised gas phase temperature versus time curve in a fire resistance testing furnace [7-9]. Such thermal exposures are commonly referred to as 'standard fires'; for purposes of this paper all mentions of standard fire exposure refer to one sided exposure to the cellulosic standard temperature-time curve defined by ISO 834 [10].

Mass timber elements like wooden beams and columns have historically been considered to demonstrate adequate performance in fire [11] (and within the standard fire resistance design framework [12]); however, as engineered mass timber is increasingly used in ever taller buildings with more complex compartment geometries, structural fire safety becomes more critical and a better understanding of structural fire performance beyond simple pass/fail criteria is essential [6, 13-18].

When mass timber is exposed to fire its load bearing capacity is reduced by two linked processes: (1) physically by the combined influence of elevated temperature and the internal movement of water in the gas phase [19-21], and (2) chemically through the ongoing pyrolysis of wood to char, which is assumed to have negligible remaining strength; this pyrolysis process is assumed to start at temperatures of about 200 °C and be completed by about 300 °C [22]. The physical loss of strength and stiffness varies between tension, compression, and shear, of which compression is the most affected mode. At 100 °C timber in compression is assumed to have lost 75 % and 65 % of its strength and elastic modulus, respectively [23, 24]. Thus, a marked loss of structural capacity occurs long before the chemical conversion of timber to char is complete.

CLT is often used for loadbearing walls for vertical and lateral load resistance and to provide compartment boundaries. In case of a fire this means that the CLT wall elements must maintain sufficient loadbearing capacity throughout the burning duration, and – in line with the fundamental intent of the standard fire resistance design framework [25]– during the decay/cooling phase of a fire so as to minimise the risk of internal fire spread, and ultimately prevent building collapse. This is a particular concern for buildings which may implement a defend-in-place or stay-put evacuation strategy – as is the case in residential buildings in some jurisdictions – and in buildings where any members of the fire and rescue services can be expected to be within the building during a fire's decay phase.

Glulam columns have been used in low- and mid-rise buildings for decades, and their behaviour as compression elements in fire has therefore been investigated previously [12, 26-28]. CLT walls, however, have received only limited research attention. A paucity of both data and understanding exists [29] on the structural fire behaviour of cross-laminated timber walls. Previous research using standard fire resistance testing has yielded a limited understanding of the structural behaviour of timber structures. This was in part due to difficulties in uncoupling the structural performance from the heating conditions as these are influenced by the fuel load from the timber structural material [30]. In addition, due to the high cost of standard fire testing, only limited studies have investigated the effect of manufacturing parameters, such as adhesive type and ply configuration, on the structural fire performance.

This paper describes a series of experiments designed to study the fire performance of CLT walls manufactured using different adhesive types, ply lay ups, and heating severities – including a fire decay and structural cooling phase, in which energy is redistributed within the timber section. The presented research represents a portion of the first author's doctoral thesis [31]. The targeted experimental design and results allow for a more detailed understanding to meet specific challenges [32] in fire safety engineering around designing appropriate timber structural fire systems for building use.

The following sections provide an overview of the current state of the art of knowledge on CLT structural performance in fire, the role of manufacturing parameters (adhesives and ply thickness), and the effect of the fire decay and cooling phase on the load bearing capacity of structural timber elements, which are all target parameters of the experiments described in this paper.

1.1 CLT walls fire safety

Previous experiments by Suzuki et al. [33] found that global buckling was the dominant failure mode for CLT walls in standard fire resistance tests. Schmid et al. [34], found that the reduced cross-section method (RCSM), which is currently advised to calculate the load bearing capacity of timber in the Eurocodes [24], was inadequate for predicting the fire resistance duration of CLT walls in standard fire tests. Limitations of the RCSM were also reported by Wiesner et al. [35] for non-standard heating conditions They also reported that the CLT walls with three plies and with thicker outer layers, with a configuration of 33-34-33 (mm), failed earlier than those with five plies, with a configuration of 20-20-20-20-20 (mm), since thicker outer layers in the three-ply CLT meant that a larger proportion of the overall load bearing capacity was damaged earlier by elevated temperatures. Bai et al. [36] assessed the residual load bearing capacity of three and five-ply CLT *after* standard fire exposure and found that, after 20 minutes of standard fire exposure, the three-ply CLT specimen was able to maintain a higher residual load bearing capacity than the five ply, however, after longer (40 minutes) standard fire exposures a higher load bearing capacity was measured for the five-ply CLT.

1.2 Adhesives at high temperatures

One of the key components for CLT, glulam and LVL structural elements are the adhesives used to bind them together. In general, these have been designed to provide equal or greater strength than solid timber at ambient temperatures, so that structural failure at ambient temperature by loss of adhesion or cohesion in the glue lines of laminated timber products is avoided [37]. However, research has shown that different adhesive types perform differently at elevated temperatures and/or under changing moisture conditions [38-46]. The two adhesive types considered in this paper are melamine urea formaldehyde (MUF) and one-component polyurethane (PU). Some prior studies have shown statistically significant differences in adhesion of PU and MUF at elevated temperatures; the stiffer, cross-linked MUF adhesives have been reported to display improved elevated temperature performance as compared against PU formulations [38, 40, 44, 47, 48]. It is noteworthy, however, that large variances in performance exist for different specific PU formulations [45, 49].

With respect to understanding the impacts of the use of CLT on the structural fire safety design of a building, at least two key issues associated with reductions in adhesive performance require consideration: (1) debonding, and (2) char fall-off (sometimes referred to as char delamination). The former denotes the loss of adhesion between two timber boards whereas the latter describes the fall off of char from timber predominantly at the adhesive line. These two phenomena may interact, with the former sometimes causing the latter. Loss of composite action due to debonding reduces the load bearing capacity of CLT elements [50-55], and the fall off of char exposes ‘fresh’ (i.e. uncharred) timber, thus increasing the charring rate and extending the burning duration [56-59].

1.3 Decay and post burn-out phases

Structural members exposed in fires must maintain sufficient loadbearing capacity not only during a fire, but also throughout the fire’s decay phase after burn out of the moveable fuel load. One of the original intents of the development of code-prescribed fire resistance ratings was to implicitly account for potential structural failure in the decay phase [60], as described in detail by Law and Bisby [25]. Recent research has explored the concern that structural failure may occur during the decay and post-burnout phases of a compartment fire due to continued heating of the timber in-depth by conduction within a timber cross-section after the peak fire temperatures have occurred. The resulting thermal wave within the cross-section can be expected to further reduce the element's structural capacity, possibly leading to collapse sometime *after* a fire has reached peak temperatures or even after it has been extinguished [61-63].

Compartment fire tests have also shown that specific CLT slabs in bending were able to initially survive burnout fires, but that one specimen eventually failed under sustained load of 5 % of its ultimate ambient capacity, due to ongoing timber smouldering [16]. This failure was observed 29 hours after the fire had burnt out. Plate thermometer measurements had reduced to 85 °C at the point of burnout, 250 minutes after ignition. Recent studies by Hirashima et al. [64] have presented post heating failure of glulam columns under sustained loads after various durations of standard furnace testing. Temperatures in-depth within the columns were observed to continue to increase for 10 hours after the fire, due to a combination of ongoing timber smouldering and conductive heat transfer. Gernay [63] applied numerical modelling to timber column data by Stanke et al. [65] and showed that the burnout resistances fell into a range between 20 and 50 % of the 'standard' fire resistance, indicating that the timber columns continued to lose load bearing capacity despite a decrease in thermal exposure, i.e. when a "cooling phase" was considered. These values are significantly lower than those for concrete columns, for which the burnout resistance was estimated as being about 72 % of the 'standard' fire resistance [66].

In CLT, the thermal penetration of both the whole wall assembly and of the individual plies are important considerations and their magnitude will depend on the external heating conditions and the material properties of the individual layers. No targeted studies on the post heating structural capacity of CLT walls exist, to the authors' knowledge.

2 Methodology

To address the knowledge gaps outlined above, a custom-made loading and simultaneous heating set-up was constructed to carefully control thermal and mechanical boundary conditions. The objective of this set-up was to illuminate the thermo-mechanical behaviour of CLT walls made from the same timber but with different adhesive types and ply thicknesses. Different radiant heating durations and intensities were chosen to assess time to failures and consequences of a cooling phase and of low thermal exposures. Instrumentation was carefully applied to measure in-depth temperatures and deflections. An annotated image of the set-up is shown in Figure 1 and detailed descriptions are given in the following subsections.

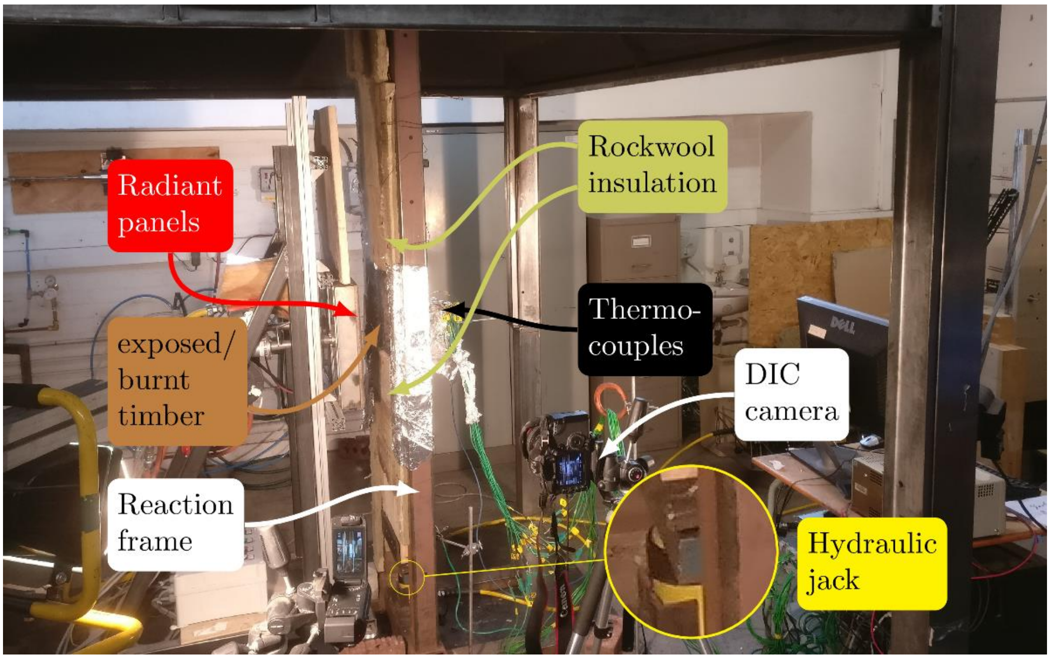

Figure 1 - Experimental set-up of the loading frame, radiant panels and instrumentation underneath an extraction hood.

2.1 Materials

The CLT used for the experiments presented herein was manufactured from *Picea abies* into CLT consisting of either three plies with thicknesses of 40-20-40 mm or five plies with thicknesses of 20-20-20-20-20 mm, thus selecting CLT wall panels that were 100 mm in thickness for both configurations. This thickness is typical of CLT products in industry (although thicker panels are possible) and has been assessed in previous tests and studies by other researchers [59, 67-69]. For both chosen configurations the fibre direction of the outer layers was parallel to the primary load bearing direction. For the five-ply system this was also true for the middle layer. The strength grades of the boards was C24 [70] with an admissible 10 % share of C16 [71]. The adhesive types used to manufacture the panels were either a one-component polyurethane (PU) adhesive or a melamine urea formaldehyde (MUF) adhesive. These parameter variations led to four combinations of ply configuration and adhesive type. All walls tested in the study presented herein were 300 mm wide and 1700 mm tall, with the outermost plies oriented vertically in both cases.

All specimens were stored in a temperature and moisture-controlled room prior to testing to ensure consistent test conditions. Oven drying on sacrificial samples showed mean moisture contents of 9 % with a standard error of 0.1 % at the time of testing. At this moisture content the specimens' mean bulk density was 463 kg/m^3 with a standard deviation of 16 kg/m^3 (the estimated coefficient of variation was 4 %).

In separate characterisation tests, published in [72], the ultimate pure compressive strength of the CLT was measured on samples with width of 100 mm, a height of 200 mm, and a depth of either 150 or 100 mm and no significant differences in compressive strength between the two adhesive types were evident at ambient temperature. The five-ply CLT was, however, observed to have a higher compressive strength than the CLT with three plies. This was attributed to a lamella effect, wherein the presence of more plies can better compensate for weaknesses in the individual timber boards [72]. The same CLT used in this study was also tested in four point bending on beams with width 300 mm, depth 100 mm, and 3000 mm length in a separate companion study [50], and no statistically significant differences were found between the two adhesive types at ambient temperatures;

however, again specimens with five plies had a higher apparent elastic modulus due to significant shear deformations occurring in the cross ply in the three-ply specimens.

2.2 Ambient temperature reference tests

Ambient temperature reference experiments were performed in duplicate for each of the four distinct CLT configurations to determine their ultimate load bearing capacity. The specimens were fitted with loading brackets at their ends and placed in a pinned-pinned vertical self-reacting loading frame (see Figure 2), and loaded under nominally concentric uniaxial compression to failure at a rate of 20 kN/min. These boundary conditions were chosen as a worst-case scenario and to minimise effects of boundary conditions on the results. Loading was imposed via a hydraulic jack connected to an inline pressure sensor and a hydraulic power pack. Lateral deflections of the walls were measured using digital image correlation [73] along with three linear potentiometers at the columns' quarter points.

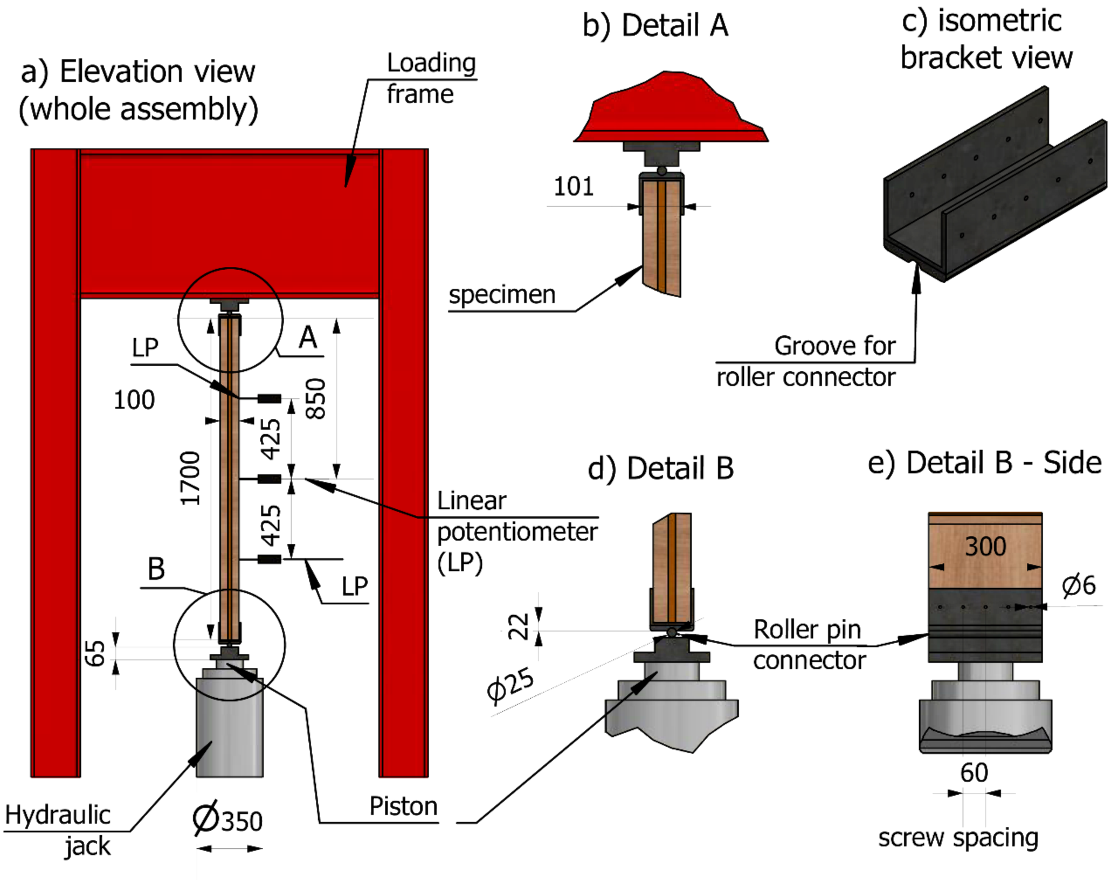

Figure 2 – Drawings of the experimental set-up for reference tests at ambient temperature conditions showing a) the elevation view of the overall set-up, b) a detail of the top connection, with dimension of the tolerance in the connector bracket, c) isometric view of the steel loading brackets, d) detailed view of the bottom connection, and e) detailed view of the bottom connection, highlighting the holes for screw fixings.

2.3 Heated Experiments

2.3.1 Loading

A custom-built reaction frame, as previously described by Wiesner et al. [35], was fitted with a hydraulic jack to apply a sustained load to the walls during heating. Two loading brackets with steel rollers slotted into matching grooves ensured pinned-pinned end connections and enabled buckling failure.; This simplified the analysis by creating an effective length factor of 1.0 for buckling. In a real building the mechanical boundary conditions may differ, which could reduce the progression of eccentricity as the cross-section is reduced due to fire exposure. Details of the loading frame and the overall experimental design are shown in Figure 3. The walls were initially loaded at ambient temperature conditions, at a rate of 20 kN/min, until the target loads of either 60.0 kN or 78.4 kN were reached, for five and three-ply CLT walls, respectively

These target loads were determined by considering the CLT manufacturers' guidance [71] on permissible ultimate loads, which are determined from calculations within EN 1995-1-1 [74] and the assumption of lateral loads of 1 kN/m^2. The resulting loads were then scaled by a factor, μ, of 0.5 for the fire situation, based on guidance in EN 1995-1-2 which recommends a value of 0.6 [24]. The slightly further reduced value of μ = 0.5 was required due the maximum capacity of the loading frame. It was decided to not vary the load ratio beyond these determined loads as this allows a better focus on the other variables investigated in this study (adhesive type, ply configuration, and heating scenario). The ultimate Euler buckling loads of the walls were calculated as 744 and 932 kN, for five and three-ply CLT, respectively.

The sustained loads applied during these experiments can be placed into context by considering recommended loads in PRG 320 [75] that deals with qualification tests for CLT; these correspond to 25 % of the allowable stress design (ADS) values. If the timber used in the current study is equivalent to quality class E1 from North America, then the recommended load would be 55.8 kN for the five-ply samples and 74.4 kN for the three-ply specimens. Hence, the applied loads of 60.0 kN and 78.4 kN used herein can be considered broadly representative of credible worst-case in-service loading conditions across various jurisdictions. Alternative calculation methods, e.g. by Thiel and Brandner [76], are available and would yield similar results under assumption of a permanent load. Herein the scaled loads from the manufacturers were used as they offered the simplest approach that avoided ambiguity of potentially inbuilt or applied safety factors.

The hydraulic power pack connected to the jack was set to maintain constant pressure once the target loads were reached. Once this was completed, the load was held at ambient temperature for a minimum of 2 minutes, and the walls were then exposed to heating as described below.

2.3.2 Thermal exposure

The walls were partially insulated (prior to loading) along their front faces and fully insulated along their side faces, limiting the area of timber directly exposed to heating to a 300 mm by 300 mm window at mid-height. An array of propane fuelled radiant panels were placed at pre-calibrated distances from the exposed area, leading to constant incident heat fluxes. This set-up was chosen to promote one-dimensional thermal gradients within the CLT walls. The area of heating was chosen as limited to the central portion to allow for better control of the thermal boundary conditions and to minimise the effect of flames from timber on the loading frame. In addition this set-up protected the pinned connections from heating, since elevated temperatures in connections were previously reported to alter the failure mode [77]. The intent of this heating set-up was not to replicate a real fire, but to impose controlled, symmetrical, experimental heating conditions that allowed elucidation of the thermo-mechanical response of the material. The chosen set-up of radiant panels allows for higher oxygen flow across the exposed timber surface, as compared to the conditions in a ventilation-controlled (i.e., Regime I) fire. Consequently, char oxidation may progress more rapidly in these experiments than in a real fire in small compartments, and thus charring rates and thermal penetrations may not be directly translatable to some real-world situations. The insulation used was 25 mm Rockwool Beamclad® [78] and was tightly fixed to the CLT using screws and washers. Insulation edges and joints were sealed using fire cement.

Three types of thermal exposure were chosen:

(1) full exposure to a 'high' heat flux with a spatial mean of 51 kW/m^2 until failure,

(2) exposure to a 'high' heat flux condition with a spatial mean of 51 kW/m^2 for a pre-determined duration with the sample subsequently allowed to cool whilst continually monitoring the thermal penetration and mechanical performance (i.e. a "cooling phase"), and

(3) a 'low' heat flux exposure of 15 kW/m^2 intended to induce smouldering without flaming combustion of the timber.

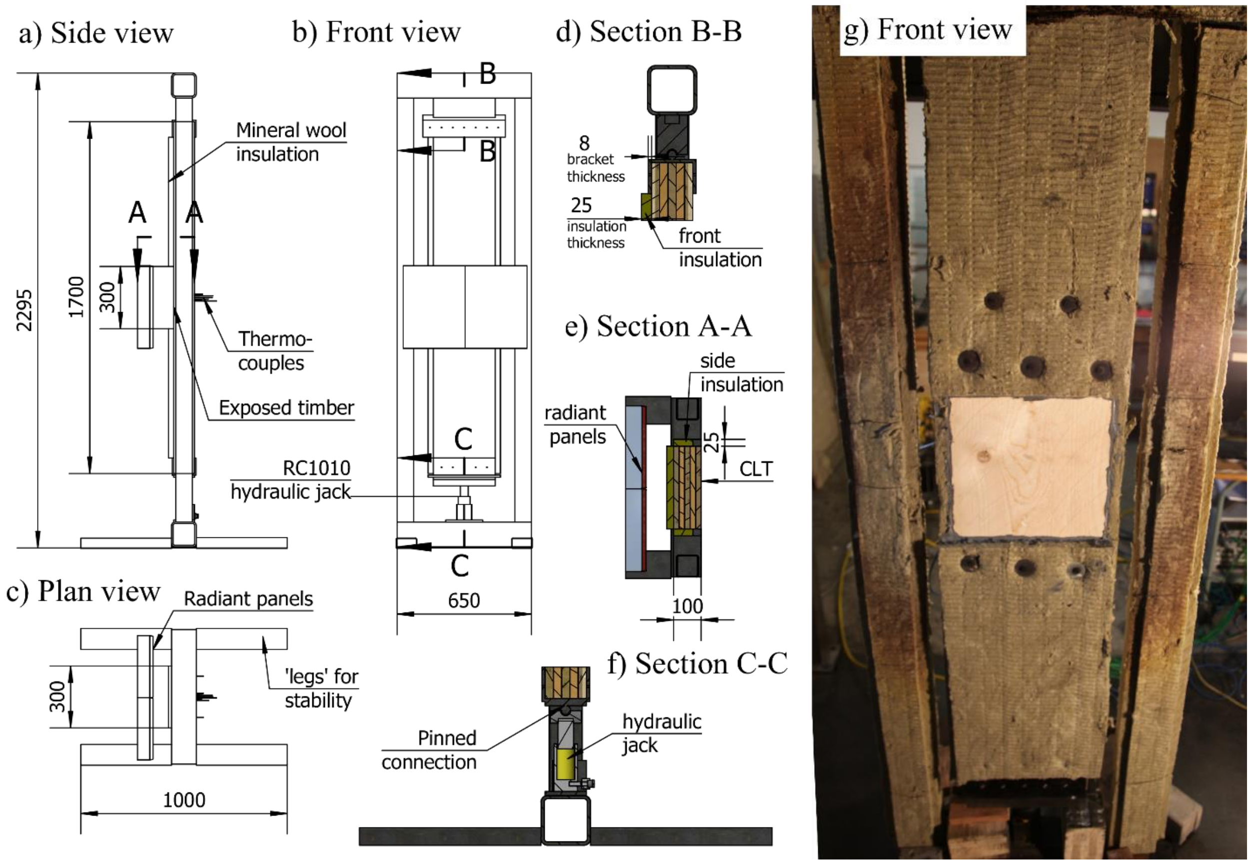

Figure 3 – Drawings of the set-up for heated experiments. a) side view of the setup, b) Front view with exposed timber obscured by radiant panels, c) plan view of the setup with stability legs, d) section view of top connection bracket and insulation detail, e) section view of central portion showing insulated CLT, f) section view of the bottom stand and connection bracket, showing hydraulic jack with extended piston., and g) photograph of exposed timber front.

A heat flux of 51 kW/m^2 is within the order of magnitude of the thermal exposures experienced in a standard fire resistance test furnace lined with brick (mean gross incident heat flux of 78 kW/m^2 over 60 minutes [79]) or expected in real compartment fires with continuous flaming [79, 80]. In addition, this thermal exposure will lead to temperature progression that is dominated by heat transfer, rather than chemical reaction rates.

The chosen lower heat flux of 15 kW/m^2 will elicit a mixed response of heat transfer and chemical reaction rates. This is relevant to assess the response of CLT walls that undergo pyrolysis in the absence of flames, this may be relevant for heating below plasterboard in encapsulated timber. In addition, past research has shown that the incident heat flux to surfaces in large, open compartment fires during traveling fires is likely to be comparatively low [81, 82].

The first specimen tested in the 'low' heat flux series (Specimen 3MF015_01) was exposed to a mean heat flux of around 21 kW/m^2; this value was used as this was the first 'low' heat flux experiment performed, and this heat flux is less than most non-piloted ignition heat fluxes for timber cited in literature [83]. Initially, no ignition or flaming was observed for this specimen (as intended); however, after five minutes of heating a small piece of char spalled off the specimen, bounced off the radiant panels, and ignited the pyrolysis gases as it bounced back towards the specimen surface, thereby causing ignition followed by flaming combustion. This unexpected ignition mechanism introduced an unwanted element of uncertainty, and it was therefore decided to reduce the heat flux for subsequent specimens to an average incident radiant heat flux of 15 kW/m^2.

The selected duration of the limited duration heat flux tests in (2) were informed by results of the high heat flux tests in (1). These heating durations were 15 and 25 minutes for three- and five-ply CLT, respectively, and corresponded to approximately 75 % of the minimum observed exposure times to failure under sustained heating of the same severity. This excluded the possibility of failure during the heating period and would yield a controlled artificially induced cooling phase. The different thermal exposures used in the current experimental programme are summarised in Figure 4.

The test matrix for all experiments in this study is shown in Table 1. Individual experiments are designated by the number of plies in the specimen, the adhesive, the target heat flux in kW/m^2, and for experiments with limited duration the letter P. In addition, specific specimens are designated as either '01', or '02' at the end of the designation string to distinguish between the repeats. For example, the second repeat of a five-ply polyurethane bonded CLT wall exposed to a 'high' heat flux with limited heating duration is designated as 5PU050P_02.

Table 1 – Experimental matrix

Designation	**Number of plies**		**Adhesive**		**Heat flux [kW/m^2]**			**Heat duration**		**n**
	3	**5**	**MUF**	**PU**	**None**	**51**	**15**	**To failure**	**Limited**	
3MF	x		x		x			x		2
3PU	x			x	x			x		2
5MF		x	x		x			x		2
5PU		x		x	x			x		2
3MF050	x		x			x		x		2
3PU050	x			x		x		x		2
5MF050		x	x			x		x		2
5PU050		x		x		x		x		2
3MF050P	x		x			x			x	2
3PU050P	x			x		x			x	2
5MF050P		x	x			x			x	2
5PU050P		x		x		x			x	2
3MF015	x		x				x	x		1
3PU015	x			x			x	x		2
5MF015		x	x				x	x		2
5PU015		x		x			x	x		2

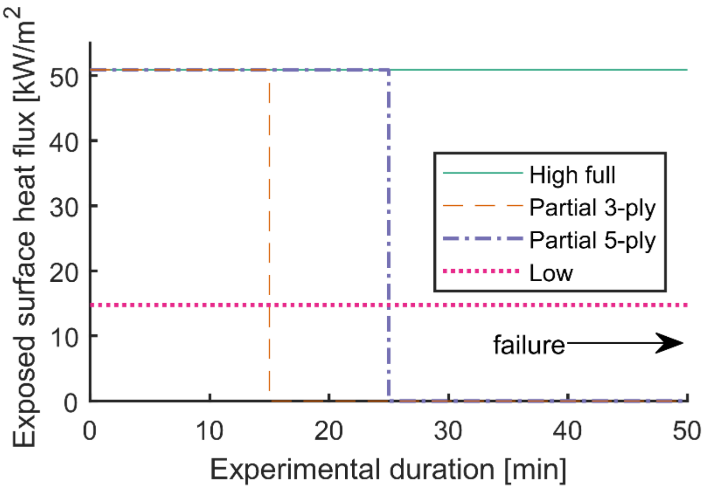

Figure 4 – Incident radiant heat flux histories and magnitudes applied in the heated tests.

2.3.3 Instrumentation

The lateral deflections of the walls were measured at five second intervals using a circle tracking scheme using digital image correlation, with targets placed on the trailing edge of the unexposed side of the walls. Details of this procedure and its validation are published elsewhere [84]. The applied loads were calculated from a pressure transducer connected to the hydraulic power pack.

Seventeen K-type Inconel sheathed Thermocouples (TCs) with a 1.5 mm diameter were placed into predrilled holes from the unexposed surface. These holes were drilled using a custom designed automated drilling system, and were 'stepped' so that the final 8 mm of each hole had a diameter of 1.5 mm whilst the remaining depth had a diameter of 2 mm. This ensured that TCs could be placed into the holes with relative ease, but would have a snug fit near their measurement tip. The in-plane locations of the TCs were arranged in a circle around a centre point, as shown in Figure 5. This arrangement was chosen so as to place thermocouples as close as possible to each other (to approximate a spot measurement at the geometric centre) whilst maintaining a minimum distance between TCs and minimise the influence of each thermocouple on its neighbours. This was done based on optimal packing density as described by Graham et al. [85], thereby achieving the highest possible proximity of thermocouples whilst maintaining a minimum spacing of 10 mm. A greater density of thermocouples was placed close to the exposed surface so as to better capture steep thermal gradients.

Due to their comparatively high thermal conductivity, Inconel sheathed thermocouples are likely to cause thermal disturbances in low thermal conductivity materials such as timber; this results in measured temperatures which are artificially lower than they would be without thermocouples present [86-88]. The temperatures and char depths presented herein were therefore corrected using a simplified procedure based on work by Beck [86] and validated against final char depths, as described by Wiesner [31].

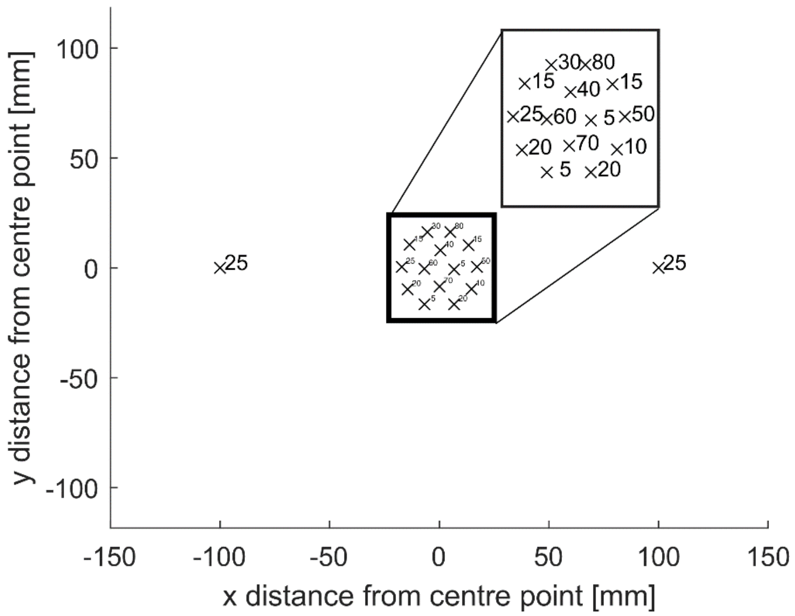

Figure 5 – Placement of thermocouples for solid phase measurements, showing location relative to centre of exposed area and placement distance from the exposed surface. The projected viewport is magnified for better readability.

3 Results

3.1 Ambient test results

All ambient temperature reference wall specimens failed due to global lateral buckling. Both the ultimate failure load and the deflection path to failure differed somewhat between tests as shown in Figure 6. The largest failure load (for sample MF_02) corresponded with minimal lateral deflection, approaching ideal Euler buckling loads before sudden lateral instability failure occurred. For specimens with low failure loads deflections occurred at lower load levels, highlighting geometric or material imperfections in the walls or inadvertent eccentricities in the placement of the mounting and loading brackets. The variation in failure loads for these experiments is considered to have been caused primarily by inadvertent initial eccentricities in the loading set-up, rather than due to underlying differences in the specimens. Such eccentricities may have arisen from the +/- 1 mm of tolerance in the loading brackets (needed to ensure that they could be mounted onto all specimens, see Figure 2 b)). Specimen MF_02 experienced a drop-in load during testing, which was caused by a sudden pressure loss, which was immediately corrected, as can be observed from the load deflection curve. An analysis of variance (ANOVA) resulted in *p*-values of 0.07 and 0.20 for adhesive type and ply layup, respectively, suggesting that any differences in load bearing capacity cannot be confidently attributed to systematic differences in the underlying population of CLT walls for this study. The absence of adhesive effects at ambient temperature is also confirmed by previous experiments on the same timber sample population in pure compression and bending [50, 72]. For the experiments with one sided heating exposure, any initial imperfections are considered unlikely to significantly influence the specimens' structural fire responses, since eccentricities induced by charring are much larger than those resulting from the mechanical loading. Compared to the measured ultimate ambient loads (which varied) the applied fire load corresponds to 10-12 % of this value.

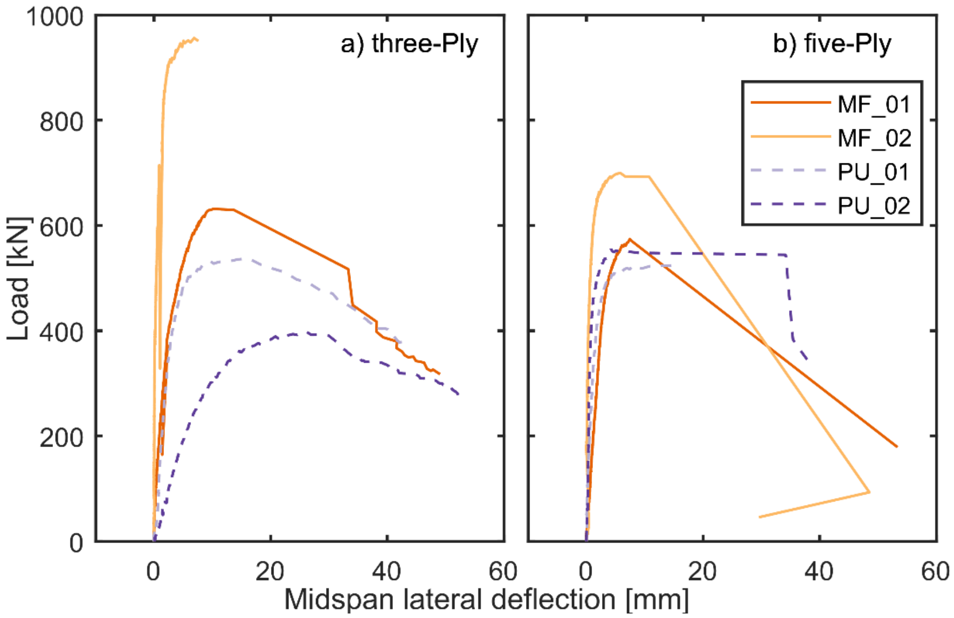

Figure 6 – Axial compressive load versus mid-height lateral deflection for ambient temperature tests for a) three-ply CLT, and b) five-ply CLT walls.

3.2 High thermal exposure

The experimentally estimated char depths and lateral mid-span deflections for CLT walls exposed to 51 kW/m^2 are shown in Figure 7 a) and 7 b), respectively. The progression of the char was estimated using an interpolated 300 °C isotherm at every timestep. The shaded areas show the 90 % confidence intervals of the char depth, determined using 1000 bootstrap (sampling *with* replacement) [89] assessments of the temperature profiles and associated 300 °C isotherm at every timestep. Char fall-off was observed for both five-ply specimens bonded with PU adhesive type.

The final measured char depth is shown by individual markers, with minimum and maximum char depths denoted with error bars. The final char depth is seen to fall within the confidence interval for most cases. No significant deviation of the char depth was observed for the char depth and rate of charring for the early stages of the fire, and only 5PU050_01 experienced a significantly higher char depth compared to the other five-ply experiments; this could have been influenced by char fall-off, which was observed only for the five-ply PU experiments.

For all specimens in Figure 7 b) structural failure is seen to be preceded by an increase in the lateral mid-height deflections. Experiments with different numbers of plies and different adhesives can be visually distinguished; three-ply specimens bonded with PU failed after 20 minutes, whilst three-ply specimens bonded with MUF failed after about 30 minutes. Failure was measured as the loss of load bearing capacity which was marked by material failure and observed from the measured pressure of the hydraulic jack. Both the deflection paths to failure and the failure times of the repeat experiments for these three-ply experiments were similar, demonstrating repeatability. For five-ply specimens the repeatability was reduced, yet the PU bonded specimens were again observed to fail earlier than those bonded with MUF. The shortest failure time for PU bonded five ply specimens was 34 minutes, for MUF bonded counterparts it was 41 minutes. The reduced repeatability for five-ply experiments is expected, because of their longer duration. This results in processes such as cracking and char oxidation having a more significant role in the heat transfer. Experiment 5MF050_01 had to be terminated prior to failure due to the insulation fasteners failing and the entire specimen becoming exposed and resulting in unsafe laboratory conditions. No insulation failures occurred in any of the other experiments.

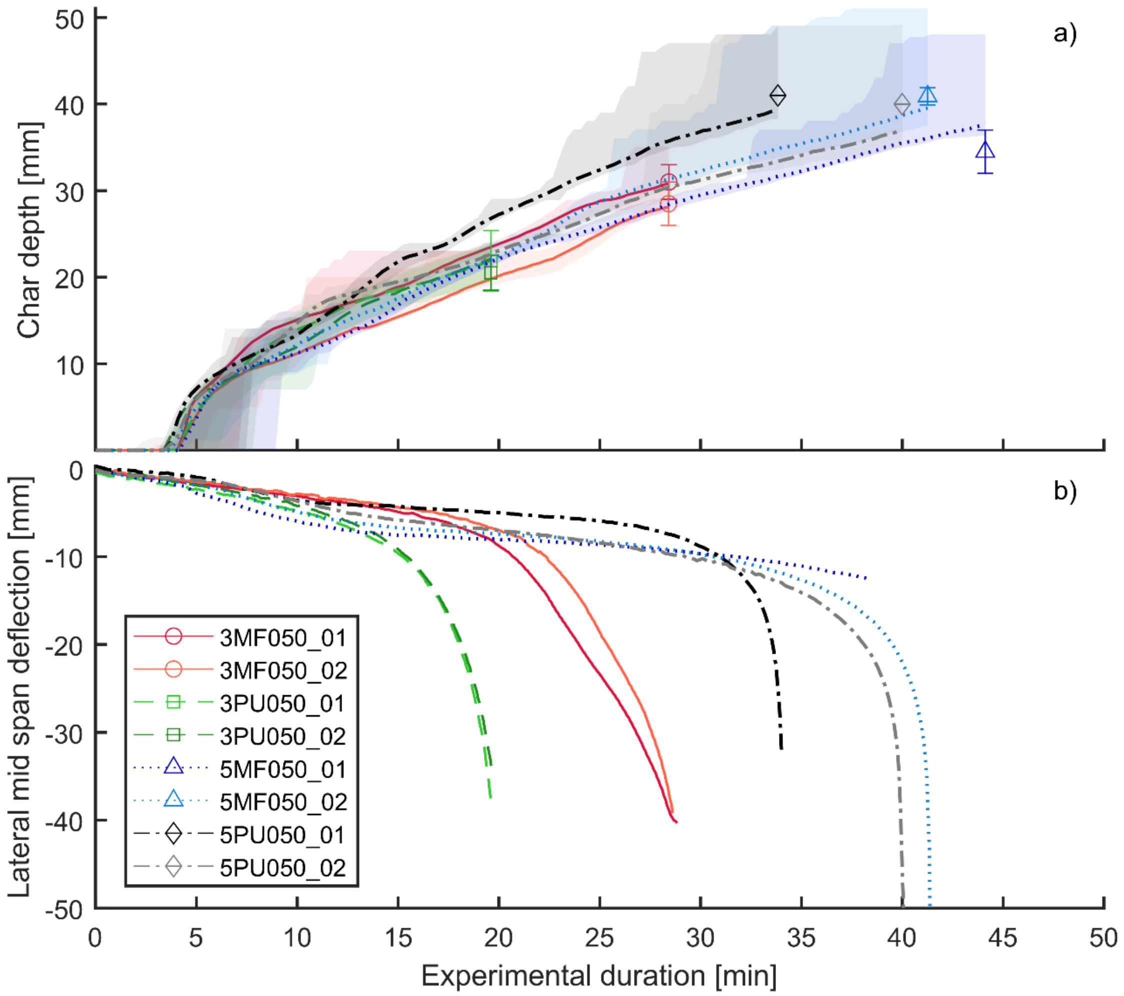

Figure 7 – a) Char depths from 300°C isotherm, and b) lateral deflections at mid height for CLT walls exposed to 'high' radiative heat flux until failure. Shaded areas show 90 % confidence intervals, markers show final measured char depth.

3.3 Limited duration heating

The typical observed sequence of events for CLT walls exposed to 'limited duration' heating is shown in Figure 8. Non-piloted ignition between 10 and 18 seconds after exposure to heating was followed by continuous flaming combustion after initial charring, and self-extinction once the incident heat flux was removed by stopping the gas supply to the radiant panels (note that the panels were left in place during cooling).

The char depths for the heating and cooling phases for the limited duration experiments are given in Figure 9 a). The radiant panels were switched off after 15 and 25 minutes for three and five ply CLT, respectively, approximately 75 % of the minimum failure time that was observed for the specimens shown in Figure 7 b). It can be seen that char progression halted when the external heat source was removed, thus highlighting self-extinction (of both flaming and smouldering) of the timber in the absence of a sufficient external heat flux. The char progression between experiments was very similar before the heat was removed.

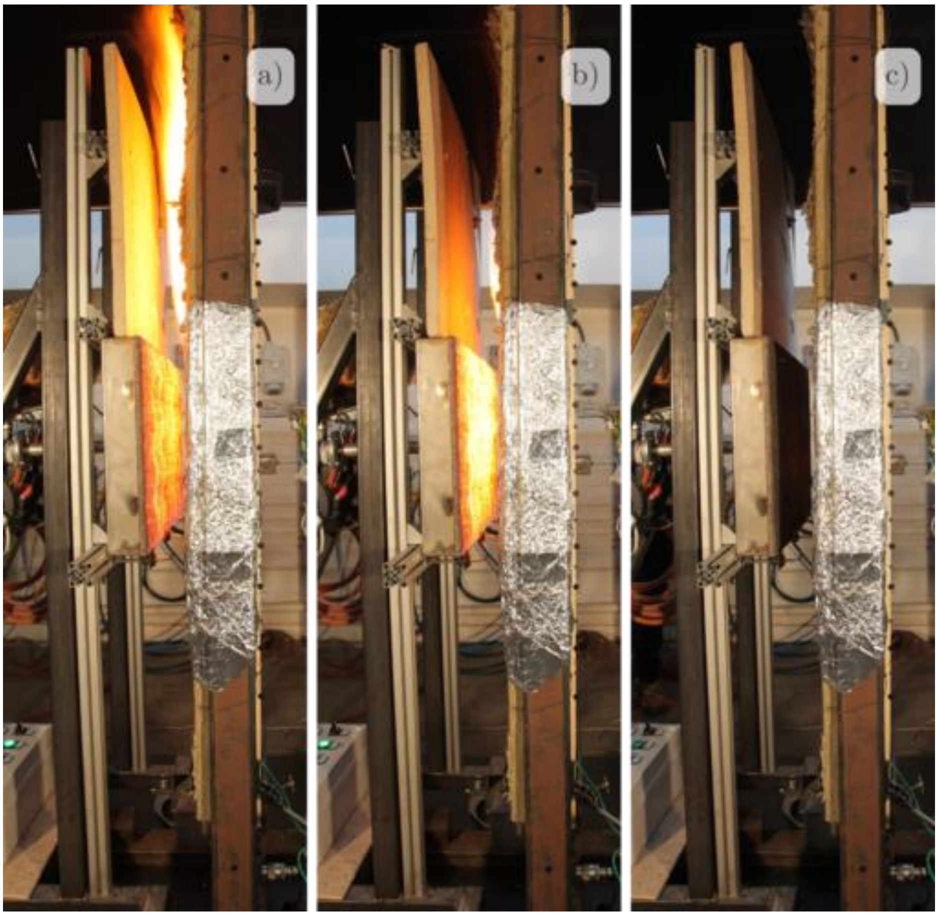

Figure 8 – Photos showing stages of experiment for walls subjected to limited duration 'high' heat flux. a) 15 seconds after heating exposure began and auto-ignition occurred, b) 10 seconds before the propane flow to the radiant panel array was halted and, c) 10 seconds after the propane flow was halted.

Figure 9 b), shows the measured deflections for CLT specimens with a cooling phase. For three-ply CLT, the radiant panel array was switched off after 15 minutes of heating, at which point the rate of deflection decreases, followed by a long duration of continuous but mild deflection increase until the experiments were eventually terminated without structural failure occurring after more than three hours. For five-ply CLT, the radiant panel array was switched off after 25 minutes. At this point, for some tests, a temporary reduction in the deflection rates was observed; however, this was followed by continuously increasing deflections leading eventually to global buckling failure for all four specimens. Five-ply PU bonded specimens failed significantly earlier than those bonded with MUF adhesive, and the variance between the two adhesive types was larger than within the adhesive types. For the three-ply specimens it was observed that the PU bonded specimens experienced higher deflections than those bonded with MUF adhesive.

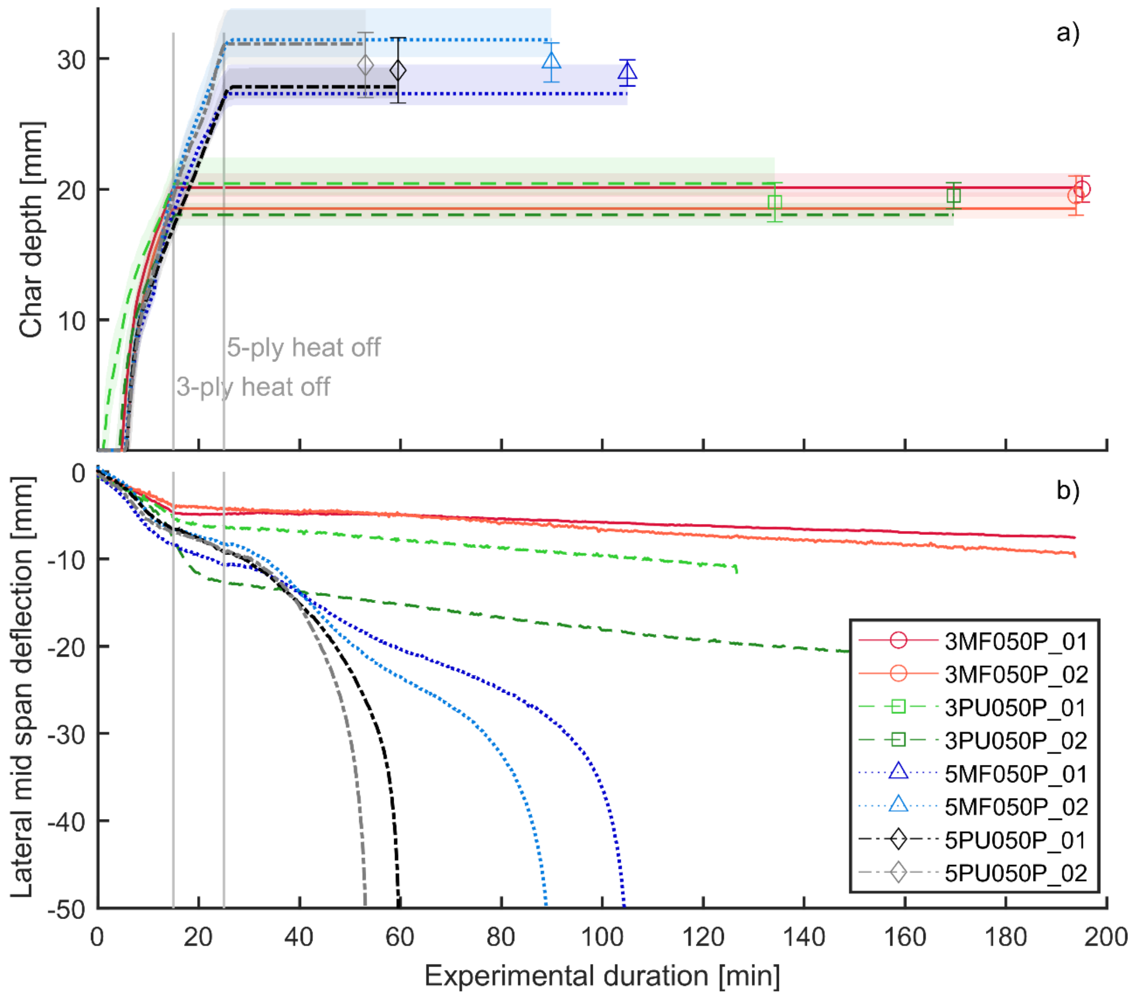

Figure 9 – a) Char depths from 300°C isotherm, and b) lateral deflections at mid height for CLT walls exposed to 'high' radiative heat flux for a limited duration with a subsequent cooling phase. Shaded areas show 90 % confidence intervals of char depth, markers show final measured char depth.

3.4 Low heating

Char progression and associated lateral deflection paths during heating for specimens heated with a sustained imposed incident radiant heat flux of 15 kW/m^2 (i.e. a 'low' heat flux) are given in Figure 10 a) and b), respectively. The times to failure were double or more those that were measured for the CLT walls that were exposed to a 'high' heat flux (see Figure 7 b). For the low heat flux tests, flaming was only observed for specimens comprising five plies using PU adhesive; for these specimens localised char fall-off occurred, leading to flaming combustion from the areas of subsequently exposed uncharred timber, which eventually self-extinguished after 7 minutes. The localised char fall-off and flaming also explains the relatively large difference in final char depth and estimated char depth presented in Figure 10 a), although the final char depths were within the 90 % confidence interval for the location of the 300 °C isotherm.

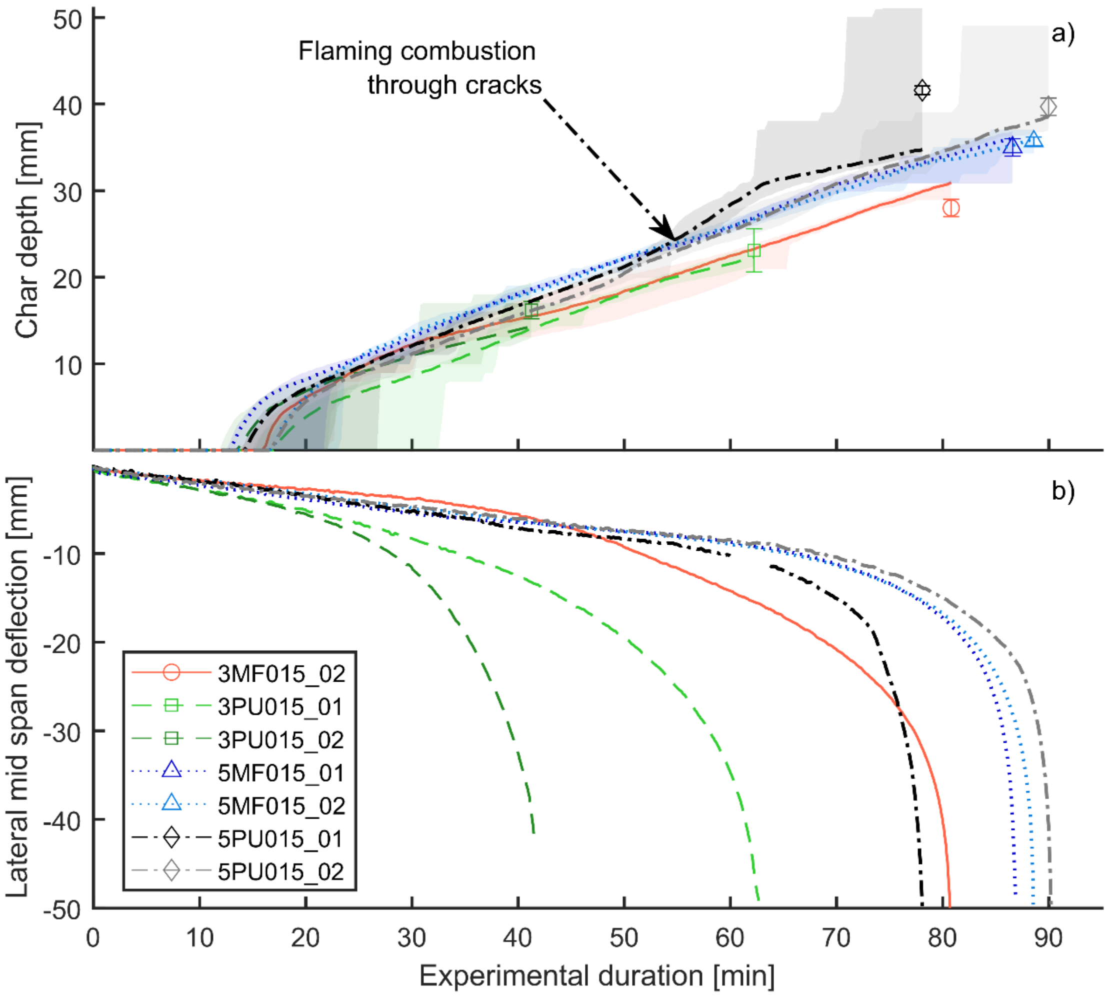

Figure 10 – a) Char depths from 300°C isotherm, and b) lateral deflections at mid height for CLT walls exposed to 'low' radiative heat flux until failure. Shaded areas show 90 % confidence intervals of char depth, markers show final measured char depth.

4 Discussion

4.1 Effect of adhesives

The results from the experiments presented in the preceding section show, based on Figures 7, 9, and 10, that CLT bonded with PU adhesive sustained larger deflections for a given thermal exposure severity and duration, resulting in shorter times to failure than when MUF adhesive was used, both for three and five-plies. The effects of adhesive differences are particularly evident in Figure 7 b) showing the lateral deflection for 'high' heat flux exposure until failure. Specimens with either adhesive type exhibited repeatability for nominally identical repeat experiments. Failure for the MUF bonded three-ply CLT sample (at 30 minutes of heating) occurred 10 minutes later than for the PU bonded sample (at 20 minutes of heating); an increase of 50 %. The close alignment of these repeat experiments suggests that potential variability in the timber is unlikely to have caused this difference. The only difference in experimental parameters between these experiments was the adhesive type, so the data provide supportive evidence that failure was caused by differences in thermal performance of the adhesive types. While it is known that different adhesives exhibit different thermal performance, the significant effect of structural performance has not previously been highlighted.

4.2 Effect of ply configuration

Irrespective of adhesive type, three-ply CLT specimens failed earlier than five-ply samples, despite similar in-depth char progression. The more pronounced deflections and earlier failures of the three-ply specimens can be explained by the absence of a cross-wise, 'sacrificial' layer in the first 40 mm of load bearing timber; which is deteriorated by the progressing thermal, moisture, and pyrolysis fronts)

In the five-ply configuration, almost one third of the total load bearing capacity is directly exposed to the fire before the structurally weak orthogonal layers temporarily reduce the rate of global load bearing capacity losses. For the three-ply configuration, the outer ply represents almost 50 % of the total load bearing capacity and experiences significant heat induced deterioration from the outset in the experiments presented herein. This also means a more rapid shift of the neutral axis of bending and subsequent more significant secondary bending (i.e. P-delta) effects.

Thicker parallel (i.e. stiffer) timber layers will also cause larger shear stresses [90, 91] within the section and along the bond lines, which will amplify the effects of weakening adhesive bond strength on the structural load bearing capacity. This will further reduce composite action, which in turn will further reduce the global axial-flexural stiffness, thus increasing lateral deflections and ultimately contributing to earlier failure. This loss of composite action has previously been observed by Wiesner et al. [50] for CLT beams (with the same adhesives and ply configurations) subjected to sustained four-point bending at temperatures up to 150 °C.

The increased lateral deflections and reduced load-bearing capacity of CLT with thick outer layers epitomizes a structural fire engineering paradox for fire-exposed load-bearing CLT elements: thicker outer layers are desirable for ambient temperature conditions, from a structural mechanics perspective, as they place more load bearing timber further from the neutral axis. In addition, from a fire dynamics perspective, thicker outer layers are likely to result in delayed char fall-off [57, 69]; this was also observed in the tests herein. This increases the likelihood that self-extinction can be achieved in a timber compartment after burn out of the moveable fuel load. For *structural fire* safety, however, the thicker outer layer leads to a reduced structural capacity in fire (compared to more thinner layers). Thus, structural fire safety should be considered explicitly, rather than as a combination of ambient temperature performance and considerations of fire dynamics.

Char fall-off was observed only for five-ply PU bonded specimens across for all thermal exposures. Three-ply PU specimens either failed before char fall-off occurred or heating was stopped before charring reached the bond line. Despite the char fall off, char progression did not deviate significantly between experiments within the same heating regimes, at least not to the point that the different structural outcomes could be explained solely by differences in char progression.

The fact that the three-ply specimens tested under full 'high' heat flux (see Figure 7 b) showed distinct structural performance, *despite* the absence of char fall-off in these experiments, strongly suggests that the adhesive performance was a relevant parameter prior to char fall-off, as well as an important consideration beyond relevant thermal exposure.

4.3 Effect of adhesive and plies across heating exposures

The three different thermal exposures created different heat transfer conditions within the tested CLT walls, and it is thus not straightforward to draw direct comparisons between the results with respect to their structural fire performance. However, the times to failure can be normalised within each exposure group by dividing them by the mean failure time for each experimental series (i.e. 'high', 'limited duration' and 'low' heat flux exposure). The resulting normalised values can then be compared across exposures.

The margins of normalised performance are shown in Figure 11, separated by the four variable configuration parameters. A value of zero indicates that a particular theoretical specimen would represent the mean performance within its group, and negative and positive margin values indicate below and above average performances, respectively. Three-ply PU bonded specimens had below average mean performance, while five-ply MUF bonded samples exhibited above average performance. These data, and p-values of 0.004 and 0.001 for adhesive type and ply layup, respectively, arising from ANOVA of the relative failure times, confirm the visual interpretation of Figure 11: the difference in structural performance between PU and MUF bonded specimens, as well as between three-ply and five-ply specimens, is considered to be statistically significant (i.e. not caused by random variation within the underlying populations).

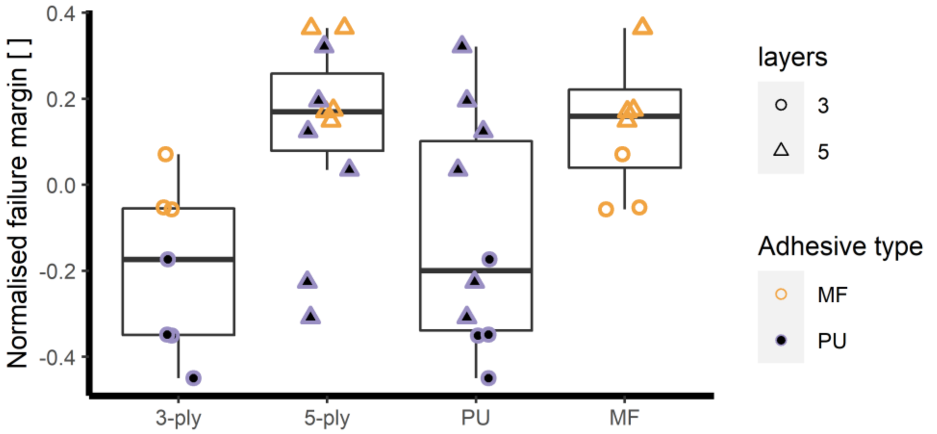

Figure 11 – Boxplot and individual datapoints of adhesive type and ply configuration for the margin of deviation of measured failure time from the normalised mean failure time within the experimental groups.

The above observations mean that the adhesive type and ply configuration have practical implications for structural fire safety and should be considered when cross-laminated timber elements are selected by structural engineering designers. Considering the failure times for individual specimens tested under ‘high’ heat flux exposures (see Figure 7 b)), it appears that the time that load bearing capacity is maintained under heating can be increased from 20 minutes to more than 40 minutes, simply by a change of adhesive type (from PU to MUF) *and* the use of five plies instead of three. It should also be considered that the majority of the five-ply PU specimens showed failure times above the mean failure time within their group. When considering individual specimens in figures 7b) and 10b) it can be seen that five-ply PU specimens may perform as well or better than those bonded with MF. Thus, polyurethane adhesive types may lead to equivalent performance as melamine formaldehyde bonded samples, if char fall-off or its effects on the charring rate ca be minimised. However, this is not the case for three-ply configurations.

The work presented in this paper provides new knowledge for manufacturers and designers seeking to optimise the design of CLT buildings, whilst also adequately considering safety, health, cost, manufacturing, and other considerations.

4.4 Failure during ‘cooling’

In tests with a forced cooling phase, the outcomes of which are detailed in subsection 3.3, specimens bonded with five plies were observed to fail after the external heat source was removed, following an exposure duration equal to 75 % of the duration required to cause failure under constant exposure. None of the three-ply samples failed under a similar condition. From Figure 9 a) the char progression halted when heating was removed, so the failure in this case was likely caused by loss of strength and stiffness associated with continued penetration of the thermal and moisture waves into the timber. This is an expected behaviour when subjecting thermally thick objects to one-sided heating.

The fact that only the five-ply samples, but none of the three-ply samples, failed is considered noteworthy, given that both sample sets were exposed to the same fraction (0.75) of their minimum expected time to failure from full 'high' heat flux exposure experiments, especially when considering that the three-ply specimens have a normalised lower performance, if tested to failure. This highlights a non-linear relationship between exposure duration and failure in the 'cooling' phase, and indicates that higher fuel loads and longer fires in timber compartments are more likely to lead to a structural *point of no return*, where deflections incurred during the fire's steady burning phase may have reduced the stability of the walls sufficiently so that further disturbances (i.e. any further material deterioration, or changes in load) could cause instability and failure.

Timber stiffness losses from heat and moisture movement are irrecoverable [50] under sustained loads, and therefore timber will not regain its structural capacity when cooled. In addition, heat and moisture movement to initially cool sections of the timber cross section will continue to weaken formerly unaffected timber and increase the likelihood of global instability of the structural element. The median in-depth temperature profiles, alongside 80 % confidence intervals, for five-ply specimens are shown in Figure 12 a) for 15 and 25 minutes of heating, before heat was removed and natural cooling induced. The thermal profiles are closely aligned; this highlights the high repeatability of the thermal exposure and suggests that the differing structural performance during the cooling phase was not caused by variation in the initial thermal exposure. Figure 12 b) shows the temperature profile of each of these specimens at the time of their structural failure alongside the median measured char depth. Due to the shorter structural failure time, the internal temperatures are higher for the PU bonded specimens in the region of the original char depth (29 to 30 mm). On the other hand, the MF bonded specimens display warmer temperatures at the unexposed surface. This arises because they fail later, so there is more time for heat to penetrate deeper into the timber, which is the cause of the ongoing reductions in structural capacity, until failure occurs. The PU bonded specimens also show lower confidence in the median temperature readings; this is caused by the occurrence of char fall-off, which creates and uneven char layer with gaps and fissures. Openings in the char layer enable higher airflow to the char, causing oxidation of the char layer and the generation of additional heat [92].

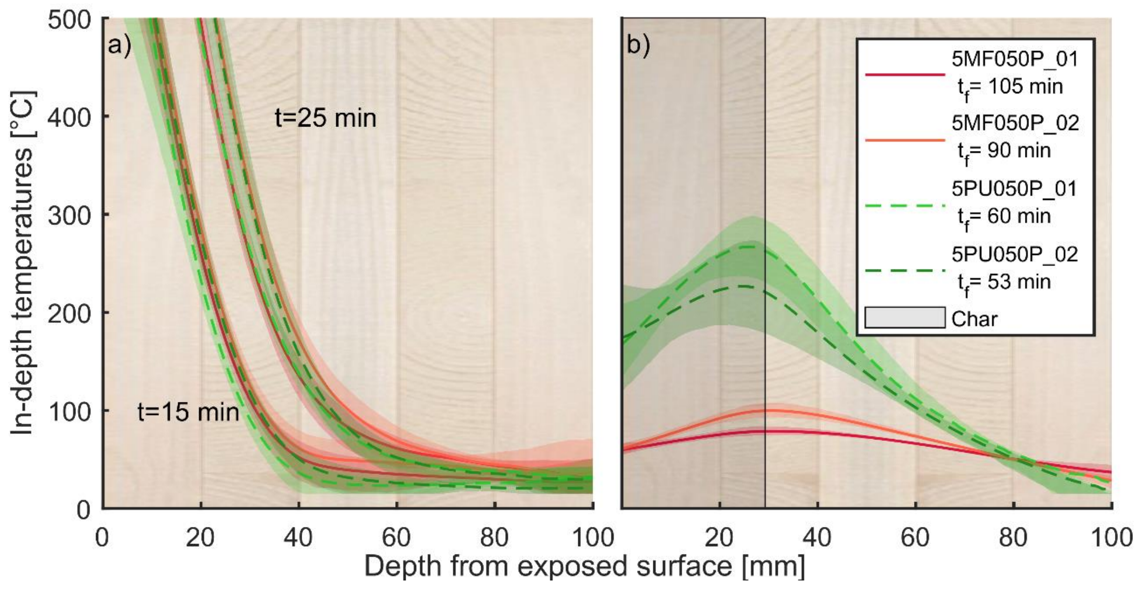

Figure 12 – In-depth CLT temperature profiles for five-ply specimens subjected to 'partial' heating for a) selected heating durations, and b) time of failure, consisting of 25 minutes heating with subsequent cooling until failure. Shaded areas denote 80 % confidence interval of temperature profiles.

In addition to the heat profiles at failure, the transient temperature readings of selected thermocouples can also be consulted for an improved understanding of the failure in the cooling phase. The charring depth for the five-ply specimens from Figure 9 a) reaches to about 30 mm from the exposed surface; this is about halfway through the second cross-wise layer, which is not assumed to contribute markedly to the load bearing capacity. The next parallel, load bearing layers are located between 40 and 60 mm, and 80 to 100 mm. Thus Figure 13a) and b) show the temperature readings for five-ply walls bonded with PU and MUF, respectively, at selected temperatures demarking the boundary of these sections. The corresponding reductions in elastic modulus, according to Eurocode 5 [24], are shown in Figure 13 b) and c) respectively. The graphs show a low continued reduction at 43 and 52 (i.e. halfway through the first remaining load bearing layer) after the heating was removed, however, this portion of timber was already reduced to almost 22 % of its original stiffness. At 62 and 63 mm a drop from approximately 50 to 35 % of residual elastic modulus can be observed, indicating a marked ongoing weakening of the second half of this parallel layer of timber. The last parallel layer, which at this point will carry the majority of the load can also be observed to undergo continued weakening after the heat was removed and charring stopped. These temperature reductions highlight that significant reductions in structural capacity of CLT walls can be expected after a fire. However, it can also be observed that the temperatures peak and cool, and the reductions therefore plateau, before failure was observed. Thus, the continued deflections and ultimate failure cannot be attributed solely to the attenuated thermal wave. Ultimately, the ongoing loss of stiffness is likely a combination of temperatures, creep (which is also linked to temperatures) and moisture movement, affecting both the timber and the adhesives. A more detailed analysis requires consideration of the overall stability of the CLT wall system and its deflections; this is out of scope of this publication but further work is ongoing.

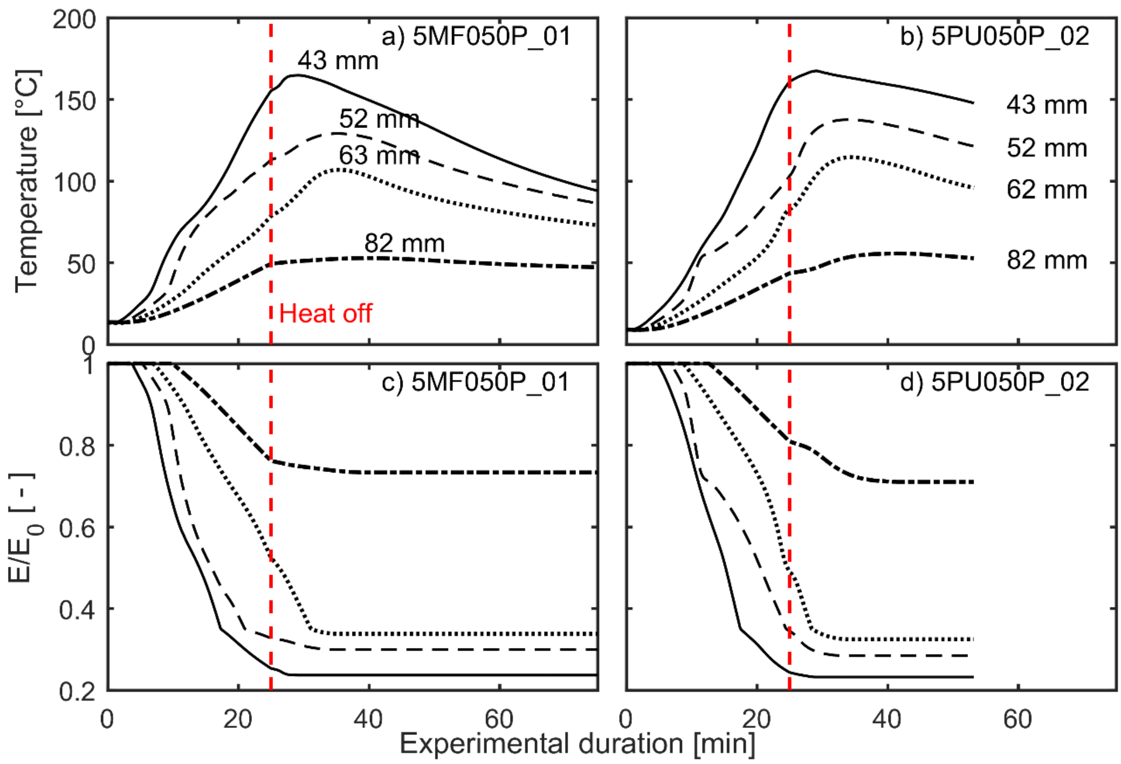

Figure 13 – Thermocouple measurements for a five-ply wall a) bonded with MUF and b) bonded with PU adhesive type. The corresponding temperature induced changes in elastic modulus according to Eurocode 5 are shown in c) and d) respectively.

Selected temperature readings and corresponding stiffness losses for three-ply CLT walls were selected based on similar reasoning as for the five-ply walls (i.e. based on remaining parallel layers) and are shown in Figure 14. The reductions in the uncharred part of the first parallel layer are severe overall, but this can be attributed to the heating phase and the losses in the cooling phase are small. The final reductions at approximately 80 mm are lower than those for the five-ply samples, which could be expected due to the shorter applied heating time.

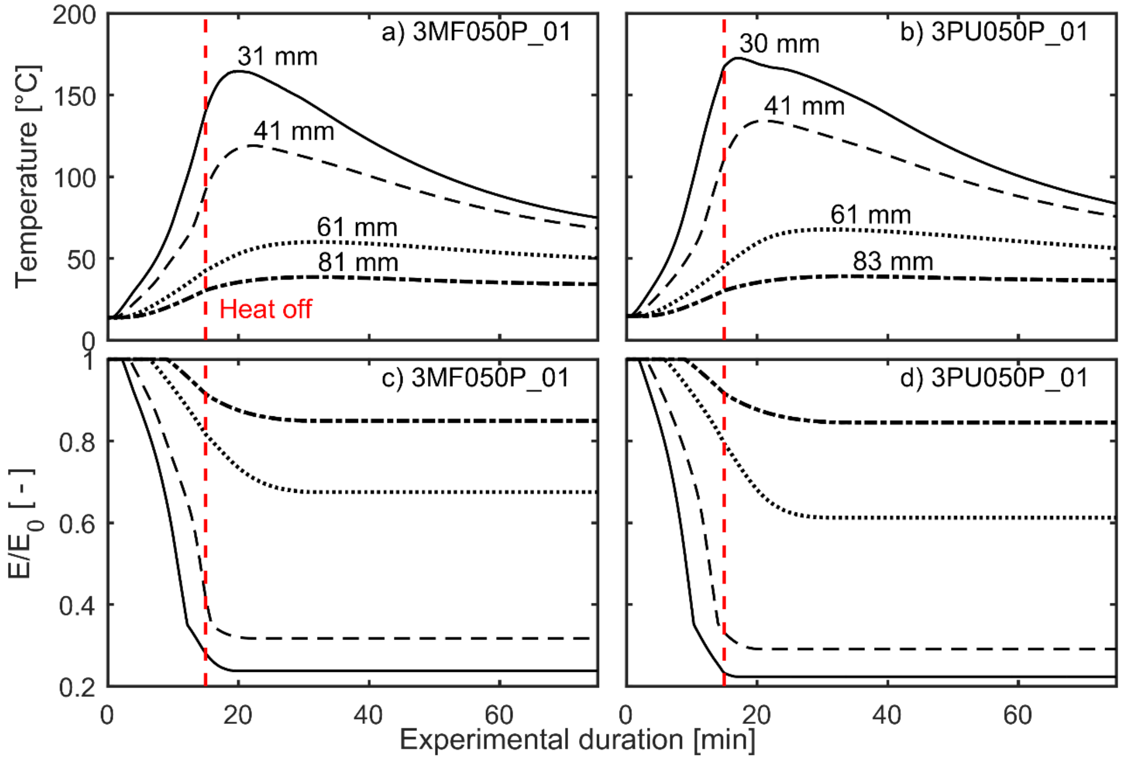

Figure 14 - Thermocouple measurements for a three-ply wall a) bonded with MUF and b) bonded with PU adhesive type. The corresponding temperature induced changes in elastic modulus according to Eurocode 5 are shown in c) and d) respectively.

The continuous slow lateral deflections of the three-ply specimens shown in Figure 9 b) suggest that these specimens could also have failed eventually, given sufficient experimental durations under sustained load; this might be caused either creep deformations or possibly ongoing smouldering in the samples at locations that were not directly instrumented. However, no signs of smouldering were visually observed for these experiments.

Structural failure of timber elements after a fire has previously been highlighted as a source of concern [61, 63, 64], yet explicit measures to address this are not currently implemented in any design guidance documents internationally. This is true for any building material.

The potential for structural failure after a fire has burned out is also a credible concern for fire and rescue operations, and for the protection of property (as determined by the building fire safety strategy). Designers should therefore endeavour to consider failure throughout all stages of a fire and until all timber has returned to ambient temperature, particularly in tall and complex buildings. Additional research on timber exposed to heating *and cooling* is therefore recommended, as is further exploration of potential smouldering combustion following mass timber compartment fires.

4.5 Failure modes

All samples failed in global buckling after experiencing rapidly accelerating lateral deflections as is evident in Figures 7, 9, and 10; this was also confirmed visually during testing. The ultimate *material* failure of the CLT walls was tensile rupture of timber on the cold side; however, the onset of runaway deflections occurred before this rupture and can be attributed to ductile yielding of heated timber in compression. Once this occurred, the bending moments in the walls increased further due to P-Delta effects. Failure was therefore governed by the reductions in compressive strength and stiffness of the timber. This is an important finding, since the majority of fire testing for CLT has focused on fire resistance of floor systems in bending where the modulus of rupture is a major contributing parameter to the load bearing capacity. In addition, widely used simplified timber fire design parameters, like the zero-strength layer, were derived from bending tests [93]. Compressive strength and stiffness are unlikely to exert major influences in bending tests, since extreme compressive stresses will only occur at the unexposed (cool) face. Thus, use of the 7 mm zero-strength layer derived from bending tests should be avoided to predict the structural fire performance of CLT walls. Instead preference should be given to advanced calculation methods that explicitly account for the loss of compressive yield strength and stiffness. The current Eurocode 5 [24], for example, includes data to enable advanced designers to do this. The results of the research presented in this paper highlight that assessment of lateral deflections of CLT walls in fire is likely to be critical to design considerations to reduce the probability of structural failure in fire.

5 Conclusions

This paper presents results from an experimental programme studying the load bearing capacity of cross-laminated timber walls exposed to heating from one side. The heating intensity, heating duration, adhesive type, and ply configuration of the CLT were varied between experiments. The heating exposure was achieved via radiant panels and the heating conditions were not directly comparable with the usual furnace testing. Instead the heating conditions created unique experimental conditions to isolate influencing parameters for structural failure in repeatable experiments.

Despite similar char progression responses, the failure times of different adhesive type and ply combinations differed significantly. Specimens bonded with PU adhesive deflected more rapidly and failed earlier than those bonded with MUF adhesive. Three-ply specimens with a ply configuration of 40-20-40 mm failed earlier than five-ply specimens with configuration 20-20-20-20-20 mm. This was attributed to the fact that in five-ply specimens, the thermal wave and pyrolysis front encountered orthogonal timber layers that did not significantly contribute to the load bearing capacity and thereby act as ‘sacrificial layers’. Based on these findings, the use of five-ply CLT is recommended to achieve higher fire performance of CLT walls.

The failure of CLT walls in the fire decay (i.e. timber cooling) phase has been empirically demonstrated through a systematic and targeted experimental program. These structural failures were observed for five-ply samples but not for three-ply samples within the test series that induced an artificial cooling phase, for which both sample groups had been subjected to heating durations corresponding to 75 % of their times to failure when tested under constant applied heating (15 and 25 minutes for three and five plies, respectively). Structural collapse in the decay/cooling phase was postulated to result from a complex interaction between thermal and structural factors wherein loading eccentricities generated during the heating phase increased the propensity for subsequent instability, in addition to structural deterioration from in-depth heating and creep deformations after the heating was halted. More research is needed to better understand the mechanical response of mass timber systems during cooling, and to provide design guidance to address the resulting concerns.

The walls failed due to global instability, with runaway lateral deflections indicating compressive yielding as the major cause of failure. Thus, loss of stiffness and accumulated lateral deflections, rather than simply a loss of material strength alone, should be considered as key considerations that may lead to structural failure for CLT walls exposed to fire. More research is recommended towards better understanding of compressive stiffness losses and deflection histories for structural fire design of CLT and other mass timber systems.

Acknowledgments

The authors gratefully acknowledge support from Ove Arup & Partners Ltd and the University of Edinburgh to undertake the experiments from which this paper draws its primary data. The authors would also like to acknowledge support from the UK Engineering and Physical Sciences Research Council (EPSRC, EP/M508032/1) and the National Centre for Timber Durability and Design Life, a collaborative research program between the University of the Sunshine Coast, University of Queensland, and the Queensland Department of Agriculture and Fisheries with financial support from Forest and Wood Products Australia. Mayr-Melnhof Holz are acknowledged for their generous contribution of materials. The authors thank Mark Partington and Michal Krajcovic for their technical assistance with the reported experiments.

References

1. Schickhofer, G., *Starrer und nachgiebiger Verbund bei geschichteten, flächenhaften Holzstrukturen* Technische Universität Graz, Fakultät für Bauingenieurwesen, 1994. **PhD**.
2. Walsh, F.J. and R.L. Watts, *Composite lumber*. 1923, U.S. Patent and Trademark Office.
3. Bergen, N.S. *Case study of UBC Brock Commons - construction details and methods*. in *World Conference on Timber Engineering*. 2016. Vienna, Austria: Vienna University of Technology.
4. Smith, R.E., G. Griffin, T. Rice, and B. Hagehofer-Daniell, *Mass timber: evaluating construction performance.* Architectural Engineering and Design Management, 2017: p. 1-12 DOI: 10.1080/17452007.2016.1273089.
5. Churkina, G., A. Organschi, C.P.O. Reyer, A. Ruff, K. Vinke, Z. Liu, et al., *Buildings as a global carbon sink.* Nature Sustainability, 2020 DOI: 10.1038/s41893-019-0462-4.
6. Buchanan, A.H. *Fire Resistance of Multistorey Timber Buildings*. in *Fire Science and Technology 2015*. 2015. Singapore: Springer.
7. Babrauskas, V. and R.B. Williamson, *The historical basis of fire resistance testing — Part I.* Fire Technology, 1978. **14**(3): p. 184-94 DOI: 10.1007/bf01983053.
8. Babrauskas, V. and R.B. Williamson, *The historical basis of fire resistance testing — Part II.* Fire Technology, 1978. **14**(4): p. 304-16 DOI: 10.1007/bf01998390.
9. Gales, J., B. Chorlton, and C. Jeanneret, *The Historical Narrative of the Standard Temperature–Time Heating Curve for Structures.* Fire Technology, 2020 DOI: 10.1007/s10694-020-01040-7.
10. ISO, *ISO 834-1-1999 Fire-resistance Test - Elements of Building Construction* in *Part 1: General requirements*. 2002, International Organisation for Standardization: Geneva, Switzerland.
11. Braidwood, Jackson, C. May, I. Anson, J. Barrett, H.A. Hunt, et al., *Discussion On The Construction Of Fireproof Buildings.* Minutes of the Proceedings of the Institution of Civil Engineers, 1853. **12**(1853): p. 266-72 DOI: doi:10.1680/imotp.1853.23988.
12. Ingberg, S.H., H.K. Griffin, W.C. Robinson, and R.E. Wilson, *Fire tests of building columns.* Journal of the Franklin Institute, 1921. **191**(6): p. 823-7 DOI: http://dx.doi.org/10.1016/S0016-0032(21)90681-1.
13. Barber, D. and R. Gerard, *Summary of the fire protection foundation report - fire safety challenges of tall wood buildings.* Fire Science Reviews, 2015. **4**(1): p. 5 DOI: 10.1186/s40038-015-0009-3.
14. Bartlett, A., F. Wiesner, R. Hadden, L. Bisby, B. Lane, A. Lawrence, et al. *State-Of-The-Art And Research Needs For Total Fire Engineering Of Mass Timber Buildings*. in *World Conference on Timber Engineering*. 2016. Vienna, Austria.
15. Bisby, L.A., J. Gales, and C. Maluk, *A Contemporary Review of Large-Scale Non-Standard Structural Fire Testing* Fire Science Reviews, 2013. **2**(1).

16. Wiesner, F., A. Bartlett, S. Mohaine, F. Robert, R. McNamee, J.-C. Mindeguia, et al., *Structural Capacity of One-Way Spanning Large-Scale Cross-Laminated Timber Slabs in Standard and Natural Fires.* Fire Technology, 2020 DOI: 10.1007/s10694-020-01003-y.
17. Naser, M.Z., *Fire resistance evaluation through artificial intelligence - A case for timber structures.* Fire Safety Journal, 2019. **105**: p. 1-18 DOI: https://doi.org/10.1016/j.firesaf.2019.02.002.
18. Hopkin, D.J., J. El-Rimawi, V. Silberschmidt, and T. Lennon, *An effective thermal property framework for softwood in parametric design fires: Comparison of the Eurocode 5 parametric charring approach and advanced calculation models.* Construction and Building Materials, 2011. **25**(5): p. 2584-95 DOI: https://doi.org/10.1016/j.conbuildmat.2010.12.002.
19. Tiemann, H.D., *Effect of moisture upon the strength and stiffness of wood*. Vol. 63. 1906: US Dept. of Agriculture, Forest Service.
20. Sulzberger, P., *The effect of temperature on the strength of wood.* Aeronautical Research Consultative. Committee Rep. ACA-46, Melbourne, 1953.
21. Gerhards, C.C., *Effect of moisture content and temperature on the mechanical properties of wood: an analysis of immediate effects.* Wood and Fiber Science, 1982. **14**(1): p. 4-36.
22. Browne, F.L., *Theories of the combustion of wood and its control*. 1958, US Dept. of Agriculture, Forest Service, Forest Products Laboratory: Madison, Wis, USA.
23. König, J. and L. Walleij, *Timber frame assemblies exposed to standard and parametric fires: part 2: a design model for standard fire exposure.* Institutet för Träteknisk Forskning, 2000(0001001): p. 1-76.
24. CEN, *Eurocode 5. Design of timber structures. Part 1-2: General. Structural fire design*. 2009, European Committee for Standardisation: Brussels.
25. Law, A. and L. Bisby, *The rise and rise of fire resistance.* Fire Safety Journal, 2020. **116**: p. 103188 DOI: https://doi.org/10.1016/j.firesaf.2020.103188.
26. Lie, T.T., *A method for assessing the fire resistance of laminated timber beams and columns.* Canadian Journal of Civil Engineering, 1977. **4**(2): p. 161-9.
27. Yoshihara, H., M. Ohta, and Y. Kubojima, *Prediction of the buckling stress of intermediate wooden columns using the secant modulus.* Journal of Wood Science, 1998. **44**(1): p. 69-72 DOI: 10.1007/bf00521877.
28. Fackler, J.P., *Essais de resistance auf feu*, in *Cahiers du Centre Scientifique et Technique du Batiment*. 1961, CSTB: Paris, France.
29. Wiesner, F. and L. Bisby, *The structural capacity of laminated timber compression elements in fire: A meta-analysis.* Fire Safety Journal, 2019. **107**: p. 114-25 DOI: https://doi.org/10.1016/j.firesaf.2018.04.009.
30. Węgrzyński, W., P. Turkowski, and P. Roszkowski, *The discrepancies in energy balance in furnace testing, a bug or a feature?* Fire and Materials, 2020. **44**(3): p. 311-22 DOI: https://doi.org/10.1002/fam.2735.
31. Wiesner, F., *Structural behaviour of cross-laminated timber elements in fires.* The University of Edinburgh, School of Engineering, 2019. **PhD** DOI: https://hdl.handle.net/1842/36675.
32. Deeny, S., B. Lane, R. Hadden, and A.T. Laurence, *Fire safety design in modern timber buildings.* The Structural Engineer: journal of the Institution of Structural Engineer, 2018. **96**(1): p. 48-53.
33. Suzuki, J.-i., T. Mizukami, T. Naruse, and Y. Araki, *Fire Resistance of Timber Panel Structures Under Standard Fire Exposure.* Fire Technology, 2016. **52**(4): p. 1015-34 DOI: https://doi.org/10.1007/s10694-016-0578-2.
34. Schmid, J., A. Menis, M. Fragiacomo, I. Clemente, and G. Bochicchio, *Behaviour of Loaded Cross-Laminated Timber Wall Elements in Fire Conditions.* Fire Technology, 2015. **51**(6): p. 1341-70 DOI: https://doi.org/10.1007/s10694-015-0516-8.

35. Wiesner, F., F. Randmael, W. Wan, L. Bisby, and R.M. Hadden, *Structural response of cross-laminated timber compression elements exposed to fire.* Fire Safety Journal, 2017. **91**(Supplement C): p. 56 - 67 DOI: https://doi.org/10.1016/j.firesaf.2017.05.010.
36. Bai, Y., J. Zhang, and H. Shen, *Residual compressive load-carrying capacity of cross-laminated timber walls after exposed to one-side fire.* Journal of Building Engineering, 2020: p. 101931 DOI: https://doi.org/10.1016/j.jobe.2020.101931.
37. Conrad, M.P., G.D. Smith, and G. Fernlund, *Fracture of wood composites and wood-adhesive joints: A comparative review.* Wood and fiber science, 2004. **36**(1): p. 26-39.
38. Clauß, S., M. Joscak, and P. Niemz, *Thermal stability of glued wood joints measured by shear tests.* European Journal of Wood and Wood Products, 2011. **69**(1): p. 101-11.
39. Clauβ, S., D.J. Dijkstra, J. Gabriel, O. Kläusler, M. Matner, W. Meckel, et al., *Influence of the chemical structure of PUR prepolymers on thermal stability.* International Journal of Adhesion and Adhesives, 2011. **31**(6): p. 513-23 DOI: https://doi.org/10.1016/j.ijadhadh.2011.05.005.
40. Kläusler, O., S. Clauß, L. Lübke, J. Trachsel, and P. Niemz, *Influence of moisture on stress–strain behaviour of adhesives used for structural bonding of wood.* International Journal of Adhesion and Adhesives, 2013. **44**: p. 57-65 DOI: https://doi.org/10.1016/j.ijadhadh.2013.01.015.
41. Kläusler, O.F., *Improvement of one-component polyurethane bonded wooden joints under wet conditions.* ETH Zurich, 2014.
42. Richter, K. and R. Steiger, *Thermal Stability of Wood-Wood and Wood-FRP Bonding with Polyurethane and Epoxy Adhesives.* Advanced Engineering Materials, 2005. **7**(5): p. 419-26 DOI: 10.1002/adem.200500062.
43. Stoeckel, F., J. Konnerth, and W. Gindl-Altmutter, *Mechanical properties of adhesives for bonding wood—A review.* International Journal of Adhesion and Adhesives, 2013. **45**(Supplement C): p. 32-41 DOI: https://doi.org/10.1016/j.ijadhadh.2013.03.013.
44. Zelinka, S.L., K. Sullivan, S. Pei, N. Ottum, N.J. Bechle, D.R. Rammer, et al., *Small scale tests on the performance of adhesives used in cross laminated timber (CLT) at elevated temperatures.* International Journal of Adhesion and Adhesives, 2019. **95**: p. 102436 DOI: https://doi.org/10.1016/j.ijadhadh.2019.102436.
45. Frangi, A., M. Fontana, and A. Mischler, *Shear behaviour of bond lines in glued laminated timber beams at high temperatures.* Wood science and technology, 2004. **38**(2): p. 119-26.
46. Zhang, R., H. Dai, and G.D. Smith, *Investigation of the high temperature performance of a polyurethane adhesive used for structural wood composites.* International Journal of Adhesion and Adhesives, 2021: p. 102882 DOI: https://doi.org/10.1016/j.ijadhadh.2021.102882.
47. Rammer, D.R., S.L. Zelinka, L.E. Hasburgh, and S.T. Craft, *Ability of finger-jointed lumber to maintain load at elevated temperatures.* Wood and Fiber Science. 50 (1): 44-54., 2018. **50**(1): p. 44-54.
48. Craft, S., R. Desjardins, and L. Richardson. *Development of small-scale evaluation methods for wood adhesives at elevated temperatures*. in *10th world conference on timber engineering*. 2008. Miyazaki, Japan.
49. Burchardt, B., *3 - Advances in polyurethane structural adhesives*, in *Advances in Structural Adhesive Bonding*, D.A. Dillard, Editor. 2010, Woodhead Publishing. p. 35-65.
50. Wiesner, F., S. Deeny, and L.A. Bisby, *Influence of ply configuration and adhesive type on cross-laminated timber in flexure at elevated temperatures.* Fire Safety Journal, 2020 DOI: 10.1016/j.firesaf.2020.103073.
51. Doyle, N., R. Emberley, and J.L. Torero. *Fire Behavior of Cross-Laminated Timber (CLT Slabs: Two-Way Action*. in *Fire Science and Technology 2015*. 2015. Singapore: Springer.

52. Emberley, R., A. Nicolaidis, D. Fernando, and J.L. Torero, *Changing Failure Modes of Cross-Laminated Timber*, in *Structures in Fire*, M.E. Moreya Garlock and V.K.R. Kodur, Editors. 2016, DEStech Publications, Inc.: Princeton. p. 643-9.
53. Smith, S.T. and J. Teng, *Interfacial stresses in plated beams.* Engineering structures, 2001. **23**(7): p. 857-71.
54. Quiquero, H., B. Chorlton, and J. Gales, *Performance of Adhesives in Glulam After Short Term Fire Exposure.* International Journal of High Rise Buildings, 2018. **7**(4).
55. Klippel, M., *Fire safety of bonded structural timber elements.* Eidgenössische Technische Hochschule ETH Zürich, Nr. 21843, 2014. **PhD**.
56. Crielaard, R., J.-W. van de Kuilen, K. Terwel, G. Ravenshorst, and P. Steenbakkers, *Self-extinguishment of cross-laminated timber.* Fire Safety Journal, 2019. **105**: p. 244-60 DOI: https://doi.org/10.1016/j.firesaf.2019.01.008.
57. Frangi, A., M. Fontana, M. Knobloch, and G. Bochicchio, *Fire behaviour of cross-laminated solid timber panels.* Fire Safety Science, 2008. **9**: p. 1279-90.
58. Hasburgh, L., K. Bourne, P. Peralta, P. Mitchell, S. Schiff, and W. Pang. *Effect Of Adhesives And Ply Configuration On The Fire Performance Of Southern Pine Cross-Laminated Timber*. in *World Conference on Timber Engineering*. 2016. Vienna, Austria: Vienna University of Technology.
59. Xing, Z., Y. Wang, J. Zhang, and H. Ma, *Comparative study on fire resistance and zero strength layer thickness of CLT floor under natural fire and standard fire.* Construction and Building Materials, 2021. **302**: p. 124368 DOI: https://doi.org/10.1016/j.conbuildmat.2021.124368.
60. Ingberg, S.H., *Tests of the severity of building fires.* NFPA Quarterly, 1928. **22**(1): p. 43-61.
61. Wiesner, F., L.A. Bisby, A.I. Bartlett, J.P. Hidalgo, S. Santamaria, S. Deeny, et al., *Structural capacity in fire of laminated timber elements in compartments with exposed timber surfaces.* Engineering Structures, 2019. **179**: p. 284-95 DOI: https://doi.org/10.1016/j.engstruct.2018.10.084.
62. Katakura, Y., H. Kinjo, T. Hirashima, S. Yusa, and K. Saito, *Deflection Behaviour and Load-Bearing-Period of Structural Glued Laminated Timber Beams in Fire Including Cooling Phase*, in *Structures in Fire*, M.E. Moreya Garlock and V.K.R. Kodur, Editors. 2016, DEStech Publications, Inc.: Princeton. p. 667-74.
63. Gernay, T., *Fire resistance and burnout resistance of timber columns.* Fire Safety Journal, 2021. **122**: p. 103350 DOI: https://doi.org/10.1016/j.firesaf.2021.103350.
64. Hirashima, T., H. Yamashita, S. Ishi, T. Igarashi, S. Baba, and T. Someya. *Deformation behaviour and failure time of glued laminated timber columns in fire*. in *The 11th International Conference on Structures in Fire* 2020. Online: School of Civil Engineering, The University of Queensland.
65. Stanke, J., E. Klement, and R. Rudolphi, *Das Brandverhalten von Holzstützen unter Druckbeanspruchung*. 1973, Bundesanstalt fuer Materialpruefung (BAM): Berlin, Germany.
66. Gernay, T., *Fire resistance and burnout resistance of reinforced concrete columns.* Fire Safety Journal, 2019. **104**: p. 67-78 DOI: https://doi.org/10.1016/j.firesaf.2019.01.007.
67. Canadian Wood Council, *Report of testing cross-laminated timber panels fo compliance with the applicable requirements of the following criteria ASTM E119-14*, in *Report Number: 101700231SAT_003*. 2014, Intertek: Elmendorf, Tx, USA.
68. Wang, Y., J. Zhang, F. Mei, J. Liao, and W. Li, *Experimental and numerical analysis on fire behaviour of loaded cross-laminated timber panels.* Advances in Structural Engineering, 2019. **23**(1): p. 22-36 DOI: 10.1177/1369433219864459.
69. Osborne, L., C. Dagenais, and N. Benichou, *Preliminary CLT fire resistance testing report.* FPInnovations, Pointe-Claire, 2012.
70. CEN, *EN 338 Structural timber - Strength classes*. 2009, European Committee for Standardisation: Brussels.

71. Mayr-Meinhof Holz Holding AG, *MM crosslam Technical Data*. 2016: Leoben, Austria.
72. Wiesner, F., D. Thomson, and L. Bisby, *The effect of adhesive type and ply number on the compressive strength retention of CLT at elevated temperatures.* Construction and Building Materials, 2021. **266**: p. 121156 DOI: https://doi.org/10.1016/j.conbuildmat.2020.121156.
73. White, D., W. Take, and M. Bolton, *Soil deformation measurement using particle image velocimetry (PIV) and photogrammetry.* Geotechnique, 2003. **53**(7): p. 619-31.
74. CEN, *Eurocode 5. Design of timber structures. Part 1-1: General. Common rules and rules for buildings*. 2014, European Committee for Standardisation: Brussels.
75. APA, *PRG 320 Standard for Performance-Rated Cross-Laminated Timber*. 2018, APA-The Engineered Wood Association: Tacoma, Washington, U.S.A.
76. Thiel, A. and R. Brandner. *ULS Design of CLT Elements – Basics and Some Special Topics*. in *Proceedings of the Joint Conference of COST Actions FP1402 & FP1404 KTH Building Materials*. 2016. Stockholm, Sweden: KTH Royal Institute of Technology.
77. Neale, J.A., *Fire Exposure Tests of Loaded Timber Columns*, in *UL Bulletin of Research*. 1939, Underwriters Laboratory: New York, USA.
78. Rockwool. *BEAMCLAD® System*. 2020 [cited 2020 12th December]; Available from: https://www.rockwool.co.uk/product-overview/fire-protection-solutions/beamclad-en-gb/.
79. Lattimer, B.Y., *Heat fluxes from fires to surfaces*, in *SFPE Handbook of Fire Protection Engineering*. 2016, Springer. p. 745-98.
80. Harmathy, T.Z., *A new look at compartment fires, part II.* Fire Technology, 1972. **8**(4): p. 326-51 DOI: 10.1007/BF02590537.
81. Hidalgo, J.P., A. Cowlard, C. Abecassis-Empis, C. Maluk, A.H. Majdalani, S. Kahrmann, et al., *An experimental study of full-scale open floor plan enclosure fires.* Fire Safety Journal, 2017. **89**: p. 22-40 DOI: http://dx.doi.org/10.1016/j.firesaf.2017.02.002.
82. Gupta, V., P. Hidalgo Juan, D. Lange, A. Cowlard, C. Abecassis-Empis, and L. Torero Jose, *A Review and Analysis of the Thermal Exposure in Large Compartment Fire Experiments.* 국제초고층학회논문집, 2021. **10**(4): p. 345-64 DOI: 10.21022/IJHRB.2021.10.4.345.
83. Babrauskas, V., *Ignition of wood: a review of the state of the art.* Journal of Fire Protection Engineering, 2002. **12**(3): p. 163-89.
84. Wiesner, F. and L. Bisby. *Robust circle tracking for deflection measurements in structural fire experiments*. in *The 11th International Conference on Structures in Fire* 2020. Online: School of Civil Engineering, The University of Queensland.
85. Graham, R.L., B.D. Lubachevsky, K.J. Nurmela, and P.R. Östergård, *Dense packings of congruent circles in a circle.* Discrete Mathematics, 1998. **181**(1-3): p. 139-54.
86. Beck, J.V., *Thermocouple Temperature Disturbances in Low Conductivity Materials.* Journal of Heat Transfer, 1962. **84**(2): p. 124-31 DOI: 10.1115/1.3684310.
87. Fahrni, R., J. Schmid, M. Klippel, and A. Frangi. *Correct Temperature Measurements in Fire Exposed Wood*. in *World Conference on Timber Engineering*. 2018. Seoul, South Korea.
88. Pope, I., J.P. Hidalgo, and J.L. Torero, *A correction method for thermal disturbances induced by thermocouples in a low-conductivity charring material.* Fire Safety Journal, 2020: p. 103077 DOI: https://doi.org/10.1016/j.firesaf.2020.103077.
89. Efron, B., *Bootstrap Methods: Another Look at the Jackknife.* Ann. Statist., 1979. **7**(1): p. 1-26 DOI: 10.1214/aos/1176344552.
90. Wiesner, F., D. Bell, L. Chaumont, L. Bisby, and S. Deeny. *Rolling shear capacity of CLT at elevated temperature*. in *World Conference on Timber Engineering*. 2018. Seoul, Republic of Korea.
91. Navaratnam, S., P.B. Christopher, T. Ngo, and T.V. Le, *Bending and shear performance of Australian Radiata pine cross-laminated timber.* Construction and Building Materials, 2020. **232**: p. 117215 DOI: https://doi.org/10.1016/j.conbuildmat.2019.117215.

92. Wiesner, F., R. Hadden, and L. Bisby. *Influence of Adhesive on Decay Phase Temperature Profile in CLT in Fire*. in *Asia-Oceania Symposium on Fire Science and Technology*. 2021. Online: The University of Queensland.
93. Schaffer, E.L., C. Marx, D. Bender, and F. Woeste, *Strength validation and fire endurance of glued-laminated timber beams*. 1986, United States Department of Agriculture, Forest Products Laboratory: Madison, WI, U.S